Scaling of the two-point velocity difference along scalar gradient trajectories in fluid turbulence

Lipo Wang
Institut für Technische Verbrennung, RWTH-Aachen, 52056 Aachen, Germany

(Received 28 August 2008; revised manuscript received 5 December 2008; published 29 April 2009)

In the context of dissipation element analysis of scalar fields in turbulence [L. Wang and N. Peters, J. Fluid Mech. **608**, 113 (2008)], the elongation of elements by the velocity difference at the minimum and maximum points was found to increase linearly with the length of an element. This paper attempts to provide a theoretical basis for this finding by analyzing two-point properties along the gradient trajectories, of which dissipation elements consist. An equation of the two-point correlation function for the product of the scalar gradient along the same trajectory can be obtained. Similar to the idea of deriving Kolmogorov's 4/5 law, there exist a scaling in the inertial range for the velocity difference, however, not same as Kolmogorov's 1/3 scaling. Specifically, by conditioning on gradient trajectories we obtain a linear relation between the velocity difference and the arclength between two points on the same trajectory. Results from direct numerical simulation (DNS) show satisfactory agreement with the theoretical prediction. This result and the derivation thereof may generally be helpful for broad stream of similar statistical and scaling studies of turbulent flows.

DOI: 10.1103/PhysRevE.79.046325 PACS number(s): 47.10.A−, 44.25.+f, 47.27.te

I. INTRODUCTION

The nonlocal behavior of turbulent fields, which can be investigated through two-point correlation functions or structure functions, remains one of the central topics in turbulence. The most prominent results derived from the Navier-Stokes equations are the Kolmogorov equation [1] for the velocity structure function and the Yaglom equation [2] for velocity-passive scalar coupled structure function, based on the assumption of isotropy.

Scalar mixing process in turbulence is of primary importance both in fundamental research and engineering applications. Geometrical properties of a scalar field, for instance, isosurface and gradient trajectories, are believed to be vital in attacking this extremely complicated problem. In the inertial range in turbulence, isosurfaces of scalars, not necessarily the passive scalar, show fractal dimensions. Sreenivasan [3] measured these dimensions experimentally for the passive scalar, vorticity, and other scalars. When scales are reduced to the level of the Kolmogorov scale, isosurfaces become smooth in a locally laminar environment. Gradient trajectories are locally normal to isosurfaces and play an important role in study the diffusion process. An interesting application of gradient trajectory is the flamelet transformation, first derived by Peters [4], presenting the variation of the scalar dissipation in scalar space, rather than in physical space. Results from Dopazo and Martin [5] have shown the significant correlation between curvature, an important shape parameter, the passive scalar, scalar dissipation, and strain rate. These results provide us abundant knowledge; however, only locally and an overall view of the entire turbulent field is still missing.

In an attempt to analyze the properties of the entire scalar fields geometrically, the concept of dissipation element has been proposed [6,7]. As illustrated schematically in Fig. 1, starting from every grid point in the passive scalar filed, the gradient trajectory can be traced in directions of ascending and descending gradients until it reaches a local maximum and minimum point, respectively. Constructed by gradient trajectories, a dissipation element is defined as the region containing all the grid points whose trajectories can share the same pair of maximum and minimum points. By definition, dissipation elements are nonarbitrarily determined and space filling. In principle, dissipation elements can be identified from various scalar fields, among which the passive scalar is of primary importance and physical interests. From the interaction of dissipation elements with vortex tubes, it shows that the orientation of dissipation elements, therefore scalar gradient trajectories, tend to be normal to vortex tubes [7], in agreement with the findings by checking the relation of eigenvectors of strain rate tensor and scalar gradient in tur-

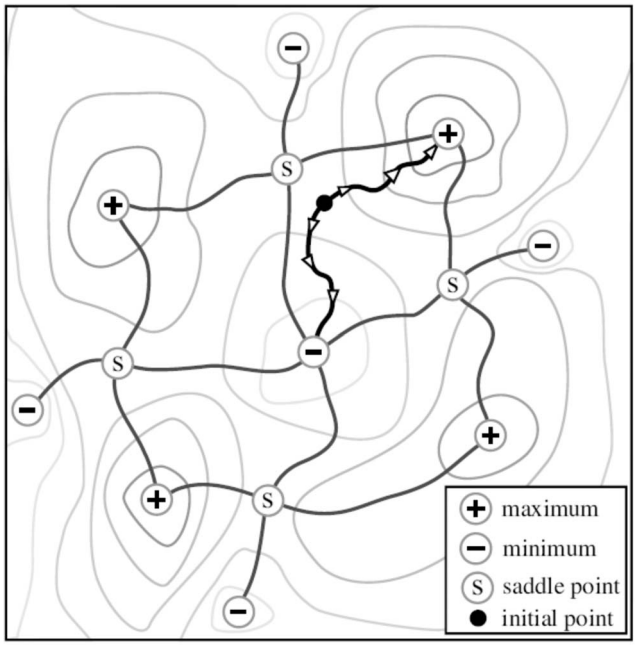

FIG. 1. Schematic illustration of dissipation elements: normal to isoscalar lines (thin solid), trajectories reach local maximal and minimal points and form dissipation elements, which are bounded by thick lines.

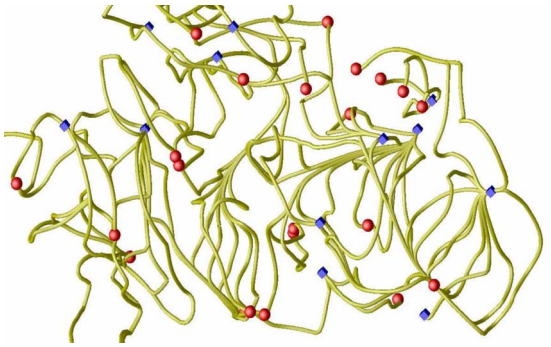

FIG. 2. (Color online) Example of gradient trajectories in a turbulent flow. Each trajectory connects one maximal [red(sphere)] point and one minimal [blue(cube)] point. Different trajectories can join at a same extremal point.

bulence [8–10]. In other words, locally the compressive strain is responsible for large scalar dissipation and the alignment of the gradient directions of the passive scalar. To quantitatively parameterize dissipation elements, two important parameters, the linear length between and the scalar difference at the extremal points, have been chosen. While as it can be expected that the conditional scalar difference follows the 1/3 Kolmogorov scaling [7], numerical data show that the velocity difference between extremal points in direction of the line connecting the extremal points surprisingly follows a linear scaling [6]. In order to explain this finding, it is meaningful to study the two-point velocity difference affixed to gradient trajectories rather than doing that in the Cartesian coordinate.

II. THEORY

In a turbulent passive scalar field ϕ, the gradient direction is $\mathbf{n}=\nabla\phi/|\nabla\phi|$. As shown in Fig. 2, in three-dimensional space gradient trajectories [(yellow) lines] have complicated geometrical shapes and their tangent directions $\mathbf{n}$ are time and space dependent. Each gradient trajectory connects one maximal [(red) sphere] point and one minimal [(blue) cube] point and thus different trajectories can join at a same extremal point. The equation governing ϕ, when written in the gradient coordinate system, becomes

$$\frac{\partial\phi}{\partial t}+u_n\phi_{,n}=D(\partial^2\phi/\partial n^2-\phi_{,n}\kappa), \tag{1}$$

where $u_n=\mathbf{u}\cdot\mathbf{n}$ is the velocity component of $\mathbf{u}$ projected on $\mathbf{n}$, $\phi_{,n}=\mathbf{n}\cdot\nabla\phi=\partial\phi/\partial n$ is the scalar gradient, n is the arclength along $\mathbf{n}$, and $\kappa=-\nabla\cdot\mathbf{n}$ is the local curvature, respectively.

Multiplying the operator $\mathbf{n}\cdot\nabla$ on both sides of Eq. (1), one obtains

$$\mathbf{n}\cdot\frac{\partial(\nabla\phi)}{\partial t}+\mathbf{n}\cdot\nabla(u_n\phi_{,n})$$
$$=\frac{\partial\phi_{,n}}{\partial t}+\frac{\partial u_n\phi_{,n}}{\partial n}=D\frac{\partial(\partial^2\phi/\partial n^2-\phi_{,n}\kappa)}{\partial n}. \tag{2}$$

Along the same trajectory, picking up another point $\mathbf{x}'$, we have similarly

$$\frac{\partial\phi'_{,n'}}{\partial t}+\frac{\partial u'_{n'}\phi'_{,n'}}{\partial n'}=D\frac{\partial(\partial^2\phi'/\partial n'^2-\phi'_{,n'}\kappa')}{\partial n'}. \tag{3}$$

The presentation of the passive scalar equation is along the gradient trajectory coordinate rather than the Cartesian coordinate. In this gradient trajectory coordinate system, the curvilinear distance between point $\mathbf{x}$ and $\mathbf{x}'$ is $l=n'-n$. Multiplying Eq. (2) by $\phi'_{,n'}$ and Eq. (3) by $\phi_{,n}$ and adding both equations together, one can take an average to obtain the two-point correlation $\overline{\phi_{,n}\phi'_{,n'}}$. As in homogenous turbulence, this statistical quantity, conditioned on gradients trajectories, is only a function of the distance l, dependent on neither n nor n'. Also taking into account that the unprimed variables do not depend on n' whereas the primed variables do not depend on n, we obtain the following equation for $\overline{\phi_{,n}\phi'_{,n'}}$:

$$\frac{\partial\overline{\phi_{,n}\phi'_{,n'}}}{\partial t}+\frac{\partial(\overline{u'_{n'}\phi'_{,n'}\phi_{,n}}-\overline{u_n\phi_{,n}\phi'_{,n'}})}{\partial l}$$
$$=D\left[\overline{\phi_{,n}\frac{\partial}{\partial n'}\left(\frac{\partial^2\phi'}{\partial n'^2}-\phi'_{,n'}\kappa'\right)}+\overline{\phi'_{,n'}\frac{\partial}{\partial n}\left(\frac{\partial^2\phi}{\partial n^2}-\phi_{,n}\kappa\right)}\right]$$
$$=D\frac{\partial}{\partial l}\left[\overline{\phi_{,n}\frac{\partial^2\phi'}{\partial n'^2}}-\overline{\phi_{,n}\phi'_{,n'}\kappa'}-\left(\overline{\phi'_{,n'}\frac{\partial^2\phi}{\partial n^2}}-\overline{\phi'_{,n'}\phi_{,n}\kappa}\right)\right]$$
$$=D\frac{\partial}{\partial l}\left[2\frac{\partial}{\partial l}(\overline{\phi_{,n}\phi'_{,n'}})-\overline{\phi_{,n}\phi'_{,n'}}(\kappa'-\kappa)\right]. \tag{4}$$

We will compare $\overline{\phi_{,n}\phi'_{,n'}}$ with the two-point correlation of the scalar gradient in the Cartesian coordinate system $\overline{\phi_{,i}\phi'_{,j}}$ and denote them by $C_{ij}(r,t)\equiv\overline{\phi_{,i}\phi'_{,j}}$ and $C_{nn'}(l,t)\equiv\overline{\phi_{,n}\phi'_{,n'}}$, respectively.

For the term C_{ij}, each component can be positive and negative, therefore the product does not need to be positive; however, for the term $C_{nn'}$, each component is positive-definite (with reference in the ascending direction along gradient trajectories) and thus $C_{nn'}$ is also positive-definite. This is the essential difference between statistics in the Cartesian coordinates and the conditional statistics in arclength coordinates. To manifest this property, two direct numerical simulation (DNS) cases for homogeneous shear turbulence with unity Prandtl number have been performed in a 2π cubic domain with an imposed mean scalar gradient $K=d\phi/dx_2=1/(2\pi)$ and other relevant parameters listed in Table I. Figures 3(a) and 3(b) show the normalized function $f_{ij}(r,t)\equiv C_{ij}(r,t)/C_{ij}(0,t)$ (using $i=1$ and $j=1$ for illustration) and

$$g(l,t)\equiv C_{nn'}(l,t)/C_{nn'}(0,t), \tag{5}$$

respectively.

It can be seen that in Cartesian coordinate system, the two-point correlation of scalar gradients are positive only up to about seven times the Kolmogorov scale η and then becomes negative tending to zero at large r/η, which means the components of passive scalar gradient are correlated only

TABLE I. Characteristic parameters of two DNS cases.

	Case 1	Case 2
Mean shear $S=d\langle v_1\rangle/dx_2$	0.5	1.5
Grid points	512^3	512^3
Viscosity ν	0.003	0.003
Turbulent kinetic energy k	0.827	2.62
Dissipation ε	0.112	0.978
Dissipation ε/k	0.135	0.373
Scalar variance $\langle\phi'^2\rangle$	0.0622	0.0290
Scalar dissipation $\langle\chi\rangle$	0.0188	0.0222
Kolmogorov scale η	0.022	0.0129
Taylor scale λ	0.471	0.283
$Re_\lambda=v_{rms}\lambda/\nu$	116.5	125.0
Resolution $\Delta x/\eta$	0.558	0.950

in the viscous diffusive range. As has been mentioned before, $C_{nn'}(r,t)$ must be positive-definite and furthermore Fig. 3(b) shows that in the inertial range $g(l,t)$ follows a scaling with respect to l as $l^{-2/3}$.

To distinguish properties of the correlation function in different ranges, we write Eq. (4) as

$$\frac{\partial[\overline{(u'_{n'}-u_n)\phi'_{,n'}\phi_{,n}}]}{\partial l} = D\frac{\partial}{\partial l}\left[2\frac{\partial}{\partial l}\overline{(\phi_{,n}\phi'_{,n'})}-\overline{\phi_{,n}\phi'_{,n'}(\kappa'-\kappa)}\right]-\frac{\partial\overline{\phi_{,n}\phi'_{,n'}}}{\partial t} \tag{6}$$

and discuss it in the inertial range and viscous diffusive range separately.

A. Inertial range

In the inertial range the viscous term can be neglected. After replacing $\overline{\phi_{,n}\phi'_{,n'}}$ in Eq. (6) by $C_{nn'}(l,t)=C_{nn'}(0,t)g(l,t)$, we obtain

$$\frac{\partial[\overline{(u'_{n'}-u_n)\phi'_{,n'}\phi_{,n}}]}{\partial l}\sim-\frac{\partial C_{nn'}(0,t)g(l,t)}{\partial t} = -g(l,t)\frac{\partial C_{nn'}(0,t)}{\partial t}-C_{nn'}(0,t)\frac{\partial g(l,t)}{\partial t}. \tag{7}$$

For steady-state turbulence $g(l,t)$ is time independent and the last term in Eq. (7) vanishes. For nonsteady flows, due to the fixed boundary conditions of $g(l,t)$, i.e., $g(0,1)=1$ and $g(\infty,t)=0$, it is still reasonable to expect the validity of a steady assumption for the normalized function $g(l,t)\equiv C_{nn'}(l,t)/C_{nn'}(0,t)=g(l)$, although both $C_{nn'}(r,t)$ and $C_{nn'}(0,t)$ are functions of time. Therefore the last term in Eq. (7) can be neglected. The $-2/3$ scaling of g in Fig. 3(b) is from the present DNS cases. There may exist different scalings for different flow conditions. Therefore we can generally assume that

$$g(l)\sim l^{-p},\quad (l_c<l<\infty), \tag{8}$$

where $0\le p\le 1$ and the reference length $l_c\sim O(\eta)$.

Integrating Eq. (7) with respect to l from l_c, we obtain

$$\overline{(u'_{n'}-u_n)\phi'_{,n'}\phi_{,n}}\sim-\frac{\partial C_{nn'}(0,t)}{\partial t}\int_{l_c}^{l}g(x)dx = -\frac{\partial C_{nn'}(0,t)}{\partial t}\left(\frac{l^{1-p}}{1-p}-\frac{l_c^{1-p}}{1-p}\right). \tag{9}$$

Dividing both sides of Eq. (9) by $C_{nn'}(l,t)$ and by noticing that $l^{1-p}\gg l_c^{1-p}$ when $l\gg l_c$, we then find a simple proportionality in the range $(l\gg l_c)$ as

$$\frac{\overline{(u'_{n'}-u_n)\phi'_{,n'}\phi_{,n}}}{C_{nn'}(l,t)}\sim-\frac{1}{C_{nn'}(0,t)}\frac{dC_{nn'}(0,t)}{dt}\frac{l}{1-p}. \tag{10}$$

In the following for comparison, two different functions

$$f_1(l)=\overline{(u'_{n'}-u_n)\phi'_{,n'}\phi_{,n}}/C_{nn'}(l,t) \tag{11}$$

and

$$f_2(l)=\overline{(u'_{n'}-u_n)} \tag{12}$$

will be introduced.

For the right-hand side of Eq. (10), physically $C_{nn'}(0,t)$ is the mean of the square of passive scalar gradient, proportional to the overall mean scalar dissipation. Thus $\frac{1}{C_{nn'}(0,t)}\frac{dC_{nn'}(0,t)}{dt}$, a function of time only, is the time rate of relative change of the overall mean scalar dissipation. The only appropriate time scale to describe overall variation processes in turbulence is the integral time τ. Thus we obtain the following relation:

$$\frac{1}{C_{nn'}(0,t)}\frac{dC_{nn'}(0,t)}{dt}\sim-\frac{1}{\tau}, \tag{13}$$

in which the negative sign on the right-hand side appears naturally from the effect of decaying on fluctuations. We may then conclude that, in the inertial range,

$$f_1(l)\sim l\frac{1}{\tau}. \tag{14}$$

From the property of scalar gradient shown in Figs. 3(a) and 3(b), the correlation length between scalar gradients is of the order of η, much shorter than that of scalar itself. This result can be understood from the fact that under the frequent compressing and stretching by the velocity field, the profile of the scalar gradient is not as smooth as that of scalar, but has wrinkles [11]. By the same token, the velocity difference $u'_{n'}-u_n$ and $\phi'_{,n'}\phi_{,n}$ will not be correlated at scales $l\gg\eta$. Thus in the inertial range $(l\gg\eta)$ it is reasonable to write

$$\overline{(u'_{n'}-u_n)\phi'_{,n'}\phi_{,n}}\sim\overline{(u'_{n'}-u_n)}\cdot\overline{\phi'_{,n'}\phi_{,n}} \tag{15}$$

and consequently

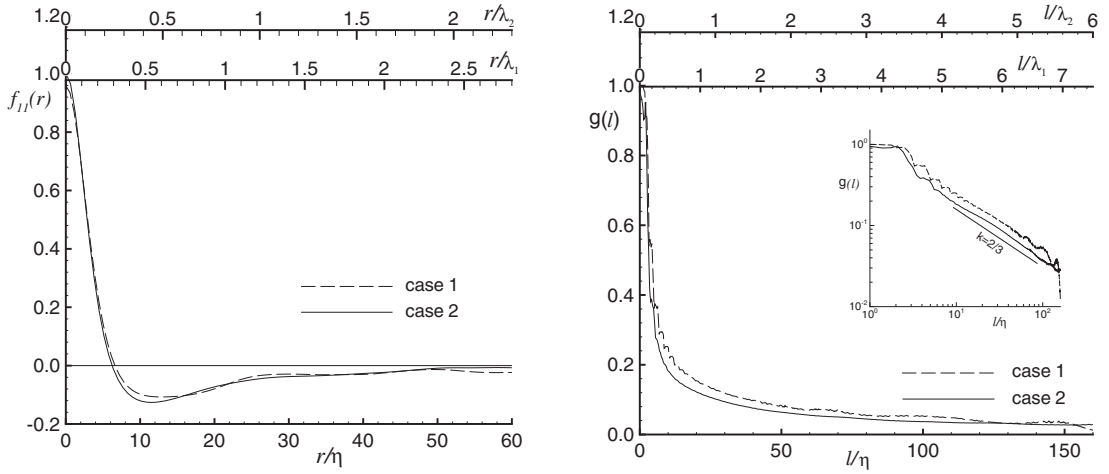

(a) (b)

FIG. 3. The correlation function: (a) $f_{11}(r)$ in the Cartesian coordinate; (b) $g(l)$ along gradient trajectories.

$$\overline{(u'_{n'}-u_n)\phi'_{,n'}\phi_{,n}}/C_{nn'}(l,t) \sim \overline{(u'_{n'}-u_n)}. \tag{16}$$

Therefore

$$f_2(l) = \overline{(u'_{n'}-u_n)} \sim f_1(l) \sim l\frac{1}{\tau}, \tag{17}$$

which tells us that at large scales velocity differences between two points along gradient trajectories increase linearly with respect to the separation arclength, different from the classical Kolmogorov 1/3 scaling for the velocity difference. Physically this difference may be understood and explained as follows. Regions with extensive strain will smooth the scalar and allow gradient trajectories to extend over a larger distance. Therefore gradient trajectories with longer arclengths mark regions of extensive strain, created by large eddies over the order of the integral time scale. Conditioning on gradient trajectories therefore extracts these regions from the entire flow filed, while unconditioned statistics in the Cartesian frame contain contributions from all strain conditions and the average of velocity difference structure function can be mixed; thus the scaling exponent is smaller than the one in the gradient trajectory coordinate system.

B. Viscous diffusive range

At small scales of the order of the Kolmogorov scalar η, the viscous term in Eq. (6) becomes dominant to lead after integration to the following balance:

$$\overline{(u'_{n'}-u_n)\phi'_{,n'}\phi_{,n}} \sim D\left[2\frac{\partial C_{nn'}(l,t)}{\partial l} - \overline{\phi'_{,n'}\phi_{,n}(\kappa'-\kappa)}\right]. \tag{18}$$

For the two terms on the right-hand side of Eq. (18), Fig. 3(b) shows that at small scales the first one $\partial C_{nn'}(l,t)/\partial l$ is negatively large (except that at $l=0$, $\partial C_{nn'}(l,t)/\partial l$ needs to be zero). Curvatures κ' and κ in the second term are important for the local diffusion. Probability density functions (PDFs) of the absolute and mean-square curvature have been checked in [12] from DNS data. Taking into consideration of the direction of scalar gradients, it was found [13] that along positive directions on average curvature increases from negative to positive. Specifically, in the vicinity of maximal points, it approaches positive infinite, while close to minimal points, tends to negative infinite. Therefore from point x to x' along the ascending direction of a same gradient trajectory $-\overline{(\kappa'-\kappa)}$, $-\overline{\phi_{,n}\phi'_{,n'}(\kappa'-\kappa)}$ as well, is negative. Thus $\overline{(u'_{n'}-u_n)\phi'_{,n'}\phi_{,n}}$ and $\overline{(u'_{n'}-u_n)}$ need to be negative at small scales in the viscous diffusive range, which is consistent with the local alignment conclusion [9] that scalar gradient tends to compressive strain direction, i.e., a negative $\overline{(u'_{n'}-u_n)}$.

III. NUMERICAL VERIFICATION

To verify the theoretical prediction in Eqs. (14) and (17), numerical analysis has been carried out from DNS case 1 and case 2. Results for f_2 and f_1 for reference as well are shown in Figs. 4 and 5, respectively. Differently from averaging in Cartesian coordinate where sample points are equally weighted, sample points along gradient trajectories are not equally volume-weighted and this weighting effect has been considered in the numerical analysis. Figures 4 and 5 show clearly the linear variation tendency of f_1 and f_2 with respect to l in the inertial range ($l \gg l_c$), in satisfactory agreement with the theoretical analysis. Furthermore, the slopes of f_2 (f_1 for reference) in Figs. 4 and 5 are approximately 0.254 and 0.707, respectively, and the ratio of which is 0.359. The integral time τ in Eq. (14) and (17) can be expressed by the kinetic energy k and energy dissipation ε as $\tau \sim k/\varepsilon$ (other expressions may only differ by some constant factors). From the values of ε/k of these two cases in Table I, we find their ratio is 0.135:0.373=0.362. This outcome that the equality of the ratio of the slopes and the ratio of ε/k between the two cases is another strong point in support of Eq. (17).

In addition, the prediction in the viscous range that the velocity difference $\overline{(u'_{n'}-u_n)}$ is negative can also be clearly

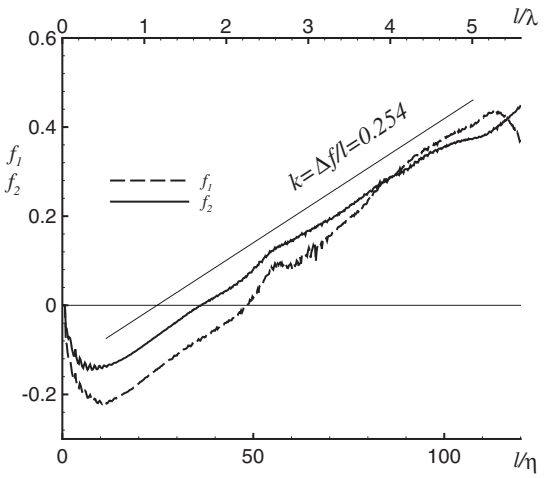

FIG. 4. Structure functions along trajectories for case 1.

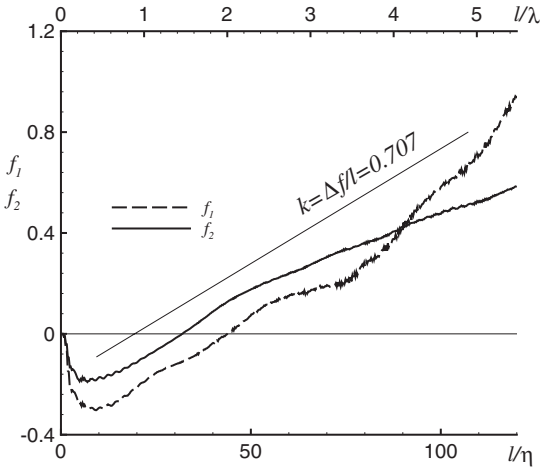

FIG. 5. Structure functions along trajectories for case 2.

observed in Figs. 4 and 5, where the negative slope parts reach approximately 10η. The negative velocity or compressive strain for small scales is an effect of diffusivity on the direction preference of scalar gradients.

IV. CONCLUSIONS

The scalar mixing process is governed by the random motion of turbulent eddies; therefore the footprint of the turbulent velocity field must be inherited, to some extent, by the signals of the passive scalar. By checking the two-point correlation of the scalar gradient and based on the fact that the triple correlation term can be decomposed [Eq. (15)], the theory introduced in this paper predicts a linear scaling of the velocity difference with the separation arclength along trajectories, which proves reasonable from numerical verifications. Compared with the classical 1/3 Kolmogorov scaling in the inertial range, the linear scaling is qualitatively different. By conditioning the statistics on gradient trajectories, regions of large extensive strain are preferentially extracted because the strain has acted on the scalar fields in a way to allow gradient trajectories to proceed over large distances. On average, the strain rate is a positive constant, except for very short elements where it becomes negative. In the Cartesian coordinate system, information along gradient trajectories may equally be partitioned into each axis and the average of velocity difference structure function can be mixed. Thus the classical scaling, i.e., 1/3, is smaller than the one in the gradient trajectory coordinate system.

When applied to study the temporal evolution of dissipation elements, this effect tends to elongate the elements such that the mean linear distance between their extremal points becomes of the order of the Taylor scale [6]. The results presented in this paper provide a theoretical explanation of Fig. 8 in [6], which helps to understand the long-distance effect of turbulent velocity on scalar trajectories. At large scales, on average, scalar gradient trajectories will be stretched, instead of being compressed as at small scales. The relations shown in Figs. 4 and 5 have similar tendency, although they are derived not from extremal points, but points along gradient trajectories. These results may also play an importance role in scalar mixing process and be helpful for statistical and scaling analysis in turbulence.

ACKNOWLEDGMENTS

The author acknowledges the motivation of this research by Professor N. Peters (RWTH-Aachen, Germany) and valuable suggestions from him. This work was founded by Deutsche Forschungsgemeinschaft under Grant No. Pe 241/38-1. The author has also benefited from Doctor J. P. Mellado (RWTH-Aachen, Germany) and Professor S. Sarkar (UCSD) in helpful discussion. HLRS at Stuttgart is appreciated for accessing NEC SX-8 supercomputer for calculation.

[1] A. N. Kolmogorov, Dokl. Akad. Nauk SSSR **32**, 19 (1941).
[2] A. M. Yaglom, Dokl. Akad. Nauk SSSR **69**, 743 (1955).
[3] K. R. Sreenivasan, Annu. Rev. Fluid Mech. **23**, 539 (1991).
[4] N. Peters, Combust. Sci. Technol. **30**, 1 (1983).
[5] C. Dopazo and J. Martin, Phys. Rev. E **76**, 056316 (2007).
[6] L. Wang and N. Peters, J. Fluid Mech. **608**, 113 (2008).
[7] L. Wang and N. Peters, J. Fluid Mech. **554**, 457 (2006).
[8] G. K. Batchelor, J. Fluid Mech. **5**, 113 (1959).
[9] W. T. Ashurst, A. R. Kerstein, R. M. Kerr, and C. H. Gibson, Phys. Fluids **30**, 2343 (1987).
[10] J. Martin, C. Dopazo, and L. Valino, Phys. Fluids **17**, 028101 (2005).
[11] C. Pantano, S. Sarkar, and F. A. Williams, J. Fluid Mech. **481**, 291 (2003).
[12] S. Pope, P. Yeung, and S. Girimaji, Phys. Fluids A **1**, 2010 (1989).
[13] L. Wang, Ph.D. Thesis, Shaker Verlag, (2008).